Vasili Yu Grishaev, Oleg I. Siidra*, Mishel R. Markovski, Dmitri O. Charkin, Timofey A. Omelchenko and Evgeni V. Nazarchuk

Synthesis and crystal structure of two novel polymorphs of (NaCl)[Cu(HSeO$_3$)$_2$]: a further contribution to the family of layered copper hydrogen selenites

https://doi.org/10.1515/zkri-2023-0004
Received January 19, 2023; accepted March 16, 2023;
published online March 30, 2023

Abstract: Crystals of two new polymorphic forms of the known compound (NaCl)[Cu(HSeO$_3$)$_2$], which we term polymorphs **II** and **III**, were formed after a *ca.* one-year dwelling of a crystalline precipitate under mother liquor and upon crystallization in the presence of K^+, respectively. Both structures belong to the "layered copper hydroselenite" family. The polymorph **II** is a structural analog of (KCl)[Cu(HSeO$_3$)$_2$] with a fully ordered Na^+ site; the main difference concerns the environment of Cu^{2+} which is more regular in (NaCl)[Cu(HSeO$_3$)$_2$]-**II**. In contrast to some expectations, crystallization from solutions containing KCl. NaCl, $CuCl_2$, and H_2SeO_3 upon evaporation does not result in formation of mixed ($Na_{1-x}K_xCl$)[Cu(HSeO$_3$)$_2$] crystals, but rather in a separate crystallization of (KCl)[Cu(HSeO$_3$)$_2$] and (NaCl)[Cu(HSeO$_3$)$_2$]-**III** which exhibits a complex structure with four ordered and one disordered Na^+ sites. It is possible that longer crystallization times enhance formation of ordered structures.

Keywords: copper; layered structures; polymorphism; selenites; [Cu(HSeO$_3$)$_2$] layers.

1 Introduction

Structural design of layered structures relies on several approaches whereof one of the most successful among inorganics relies on the use of lone-pair cations and halide anions, as well as their crystal chemical analogs (e.g. nitrates). When transition metals are involved, this often leads to compounds exhibiting low-dimensional magnetism (e.g. [1, 2]); other intriguing phenomena are expected to be manifested. Several families are hitherto known based on the stable 2D "building blocks" e.g. in arsenites, selenites, and tellurites. The two former anions can also contribute to the structure formation in partially or even fully protonated states [3–8], giving rise to hydrogen-bonded networks recently considered as "molecular inorganic polymers" [9]. Perhaps the most numerous (i.e. more thoroughly studied) is a family of copper hydrogen selenites based on [Cu(HSeO$_3$)$_2$] slabs [10–13].

Our recent study of (*AX*)[Cu(HSeO$_3$)$_2$] compounds (*A* = alkali metal, except Li; *X* = Cl, Br) has revealed that the nature of the halide anion has no effect on the structure, but the size of the cation strongly affects the interlayer (*AX*) arrangement. As a result, Na^+ and K^+ give rise to two different monoclinic structures (the latter being isostructural to (Rb*X*)[Zn(HSeO$_3$)$_2$]) [14] while the larger Rb^+, Cs^+, and NH_4^+ contribute to an orthorhombic polymorph first reported for (NH_4Cl)[Cu(HSeO$_3$)$_2$] [15]. These arrangements also differ by the copper coordination CuO_4X_n, where n = 0–2 dependent on the size of the interlayer A^+ cation.

All members of the copper hydroselenite family were prepared by the slow evaporation of strongly acidic aqueous solutions at ambient temperature which generally leads to multiphase products. This is not surprising since the respective halide (or nitrate) of monovalent or divalent cation is present in large (6- to 10-fold) excess. The target crystals are formed and exist in relatively narrow pH ranges, i.e. within a certain period of evaporation after which, at least in case of halides, they undergo various transformations [13]. In addition, copper-free compounds with peculiar structures are also

Mishel R. Markovski, Current address: Normandie Université, CNRS, Laboratoire Catalyse et Spectrochimie, 14000 Caen, France.

***Corresponding author: Oleg I. Siidra**, Department of Crystallography, St. Petersburg State University, University Emb. 7/9, St. Petersburg 199034, Russia; and Kola Science Center, Russian Academy of Sciences, Fersmana str. 14, Apatity, Murmansk Region 184209, Russia, E-mail: o.siidra@spbu.ru
Vasili Yu Grishaev, Mishel R. Markovski and Evgeni V. Nazarchuk, Department of Crystallography, St. Petersburg State University, University Emb. 7/9, St. Petersburg 199034, Russia
Dmitri O. Charkin and Timofey A. Omelchenko, Department of Chemistry, Moscow State University, Vorobievy Gory 1-3, Moscow 119991, Russia

formed at the later evaporation stages [9, 16]. Synthesis of (NaCl)[Cu(HSeO$_3$)$_2$] from freshly prepared aqueous solutions yielded blue acicular crystals of the compound first prepared in sealed silica tubes upon vapor transport [17]. However, revision of the polycrystalline mass after *ca.* one-year keeping in a closed vial (to avoid complete drying) revealed the presence of yet another type of colored crystals (yellowish green) which were found to belong to a new polymorph of the title compound. Further on, we refer to the previously described compound as to (NaCl)[Cu(HSeO$_3$)$_2$]-**I** while the new compound is referred to as (NaCl)[Cu(HSeO$_3$)$_2$]-**II**. As it was found to be isostructural to (KCl)[Cu(HSeO$_3$)$_2$] (*vide infra*), a new study was undertaken in the search of possible mixed '(NaCl,KCl)[Cu(HSeO$_3$)$_2$]' crystals. Instead, a new (third) polymorph of the sodium compound, which is named (NaCl)[Cu(HSeO$_3$)$_2$]-**III**, was serendipitously observed with another new structure type. Hereby we report and briefly discuss the structural details of these polymorphs of the (NaCl)[Cu(HSeO$_3$)$_2$] compound.

2 Experimental

2.1 Synthesis

The crystals of (NaCl)[Cu(HSeO$_3$)$_2$]-**II** were selected from the same sample whereof the crystals of previously known (NaCl)[Cu(HSeO$_3$)$_2$]-**I** were picked out [13] after ca. 1-year standing in a closed vial under small amount of mother liquor at ambient temperature. A photo of the crystals (wherein the blue ones most likely refer to (NaCl)[Cu(HSeO$_3$)$_2$]-**I**) is presented in Figure 1.

Greenish-blue single crystals of (NaCl)[Cu(HSeO$_3$)$_2$]-**III** were produced in a series of experiments aimed at possible mixed (NaCl,KCl)[Cu(HSeO$_3$)$_2$] compounds. Five starting solutions, containing 5-*n* mmol NaCl, *n* mmol KCl (*n* = 0–4), 1 mmol $CuCl_2$, and 3 mmol H_2SeO_3 in 50 ml of distilled water, were prepared. The precipitates of copper selenite were dissolved by adding 0.3–0.5 ml of trifluoroacetic acid and gentle heating for a few minutes on a hotplate (not above 45 °C). As in the previous cases, the color of the solutions changed gradually upon room-temperature evaporation from bluish to green and yellowish; green and blue acicular crystals were formed within three to five weeks.

Studies in the chemically related NaBr–KBr–$CuBr_2$–H_2SeO_3 systems did not produce any new copper-bearing compounds. The crystal structures of two new copper-free species will be reported in a separate communication.

Qualitative electron microprobe analysis of two compounds reported herein (LINK AN-10000 EDS system) revealed no other elements, except Na, Cu, Se and Cl with atomic number greater than 11 (Na).

2.2 Single-crystal X-ray studies

Single-crystal X-ray data of the new compounds were collected using a Rigaku XtaLAB Synergy-S diffractometer equipped with a PhotonJet-S detector operating with Mo*K*α radiation at 50 kV and 1 mA. A single crystal of each compound was chosen and more than a hemisphere of data collected with a frame width of 0.5° in ω, and 10 s spent counting for each frame. The data were integrated and corrected for absorption applying a multi-scan type model using the Rigaku Oxford Diffraction programs CrysAlis Pro. The structures of compounds were successfully refined with the use of Shelx software package [18]. All H atoms were located from the analysis of difference Fourier electron density maps and were refined with the imposed O–H distance restraints of 1.00 ± 0.005 Å. Atom coordinates and thermal displacement parameters are collected in the corresponding cif files (Supplementary 1); experimental parameters are provided in Table 1 and selected interatomic distances in Tables 2 and 3.

2.3 Infrared spectroscopy

The IR spectrum of (NaCl)[Cu(HSeO$_3$)$_2$]-**II** (Figure 2) was acquired at ambient conditions on a Bruker Vertex 70 FTIR spectrometer with a resolution of 4 cm^{-1}. A powdered sample was added to a dried KBr pellet using another pure KBr pellet as a reference. The band at 453 cm^{-1} can be tentatively attributed to the Cu–O stretching vibrations by analogy to the

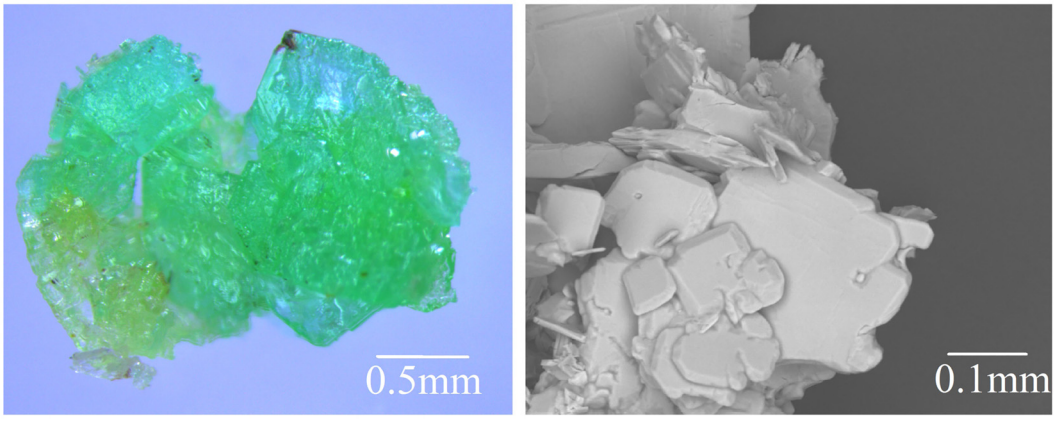

Figure 1: Mint green crystals of (NaCl)[Cu(HSeO$_3$)$_2$]-**II** overgrowing on blue crystals of (NaCl)[Cu(HSeO$_3$)$_2$]-**I** under optical microscope (left) and SEM image (right).

Table 1: Crystallographic data and refinement parameters for (NaCl)[Cu(HSeO$_3$)$_2$]-**II** and (NaCl)[Cu(HSeO$_3$)$_2$]-**III**.

Compound	(NaCl)[Cu(HSeO$_3$)$_2$]-II	(NaCl)[Cu(HSeO$_3$)$_2$]-III
Space group	*P*2/*c*	$P2_1/c$
a, Å	6.1754(5)	11.1204(3)
b, Å	5.3823(4)	29.0105(7)
c, Å	10.4442(8)	9.0128(2)
β, °	100.3420(10)	93.236(2)
V, Å^3	567.0(2)	2902.97(12)
Z	2	16
F(000)	350	2800
Radiation, wavelength, Å	Mo*K*α	Mo*K*α
Ranges of *h*, *k*, *l*	$-8 \le h \le 7$, $-4 \le k \le 7$, $-13 \le l \le 13$	$-16 \le h \le 17$, $-46 \le k \le 45$, $-14 \le l \le 9$
Number of reflections	2528	45315
Number of unique reflections	805	6474
R_1 [$F > 4\sigma(F)$]	0.014	0.038
wR_1 [$F > 4\sigma(F)$]	0.037	0.060
GOF	1.164	1.037
CCDC	2236369	2236370

Table 2: Selected interatomic distances (Å) in (NaCl)[Cu(HSeO$_3$)$_2$]-**II**.

Cu1–O2	1.9757(14) × 2
Cu1–O1	2.0291(14) × 2
Cu1–Cl1	2.6058(9)
Cu1–Cl1	2.7765(9)
Na1–O3	2.4898(19) × 2
Na1–O1	2.5426(16) × 2
Na1–O2	2.6165(16) × 2
Na1–Cl1	3.3302(6) × 2
Se1–O2	1.7026(15)
Se1–O1	1.7068(14)
Se1–O3	1.7490(16)
Se1–Cl1	3.1474(4)
Se1–Cl1	3.4530(5)

$[Cu(H_2O)_4]^{2+}$ cation [19]. The bending Cu–O vibrations lie beyond the range studied. Strong vibrations in the range 1205–787 cm^{-1} and 509 cm^{-1} correspond to the $[(HSeO_3)_2]^{2-}$ dimers linked by hydrogen bonds [20]. The Se–O stretching vibrations lie usually in the 754–679 cm^{-1} range [20, 21], while Se–OH modes are observed at 480 cm^{-1} [22]. The bands at 2829–2292 cm^{-1} correspond to O–H vibrations.

3 Results

3.1 Cation coordination in (NaCl)[Cu(HSeO$_3$)$_2$]-II

In the structure of (NaCl)[Cu(HSeO$_3$)$_2$]-**II**, the Na^+ cations are eight-coordinated and reside in polyhedra formed by six

Table 3: Selected interatomic distances (Å) in (NaCl)[Cu(HSeO$_3$)$_2$]-**III**.

Se1–O1	1.670(3)	Cu1–O2	1.955(3)	Na1–OH8	2.251(3)
Se1–O2	1.691(3)	Cu1–O9	1.963(3)	Na1–OH5	2.257(3)
Se1–OH1	1.746(3)	Cu1–O10	1.967(3)	Na1–O7	2.487(3)
Se1–Cl3	3.4860(11)	Cu1–O5	1.983(3)	Na1–O8	2.736(3)
Se1–Cl4	3.5875(11)	Cu1–Cl2	2.7180(10)	Na1–Cl1	2.881(2)
		Cu1–Cl4	2.8490(11)	Na1–Cl2	2.969(2)
Se2–O3	1.681(3)				
Se2–O4	1.690(3)	Cu2–O13	1.947(3)	Na2–OH1	2.310(3) × 2
Se2–OH2	1.738(3)	Cu2–O14	1.963(3)	Na2–O15	2.685(3) × 2
Se2–Cl3	3.3729(11)	Cu2–O4	1.970(3)	Na2–Cl3	2.8654(11) × 2
		Cu2–O7	1.981(3)		
Se3–O5	1.682(3)	Cu2–Cl4	2.6938(11)	Na3–OH4	2.272(4)
Se3–O6	1.688(3)	Cu2–Cl2	2.8702(10)	Na3–OH3	2.287(4)
Se3–OH3	1.753(3)			Na3–O9	2.546(4)
Se3–Cl4	3.5068(12)	Cu3–O11	1.940(3)	Na3–O10	2.905(4)
		Cu3–O1	1.959(3)	Na3–Cl4	2.865(2)
Se4–O7	1.685(3)	Cu3–O16	1.962(3)	Na3–Cl4	2.934(3)
Se4–O8	1.693(3)	Cu3–O6	1.977(3)		
Se4–OH4	1.737(3)	Cu3–Cl1	2.7634(10)	Na4–OH7	2.288(4)
Se4–Cl4	3.3659(12)	Cu3–Cl3	2.8543(10)	Na4–OH6	2.310(3)
Se4–Cl3	3.5796(11)			Na4–O3	2.637(3)
		Cu4–O12	1.951(3)	Na4–O5	2.804(3)
Se5–O9	1.680(3)	Cu4–O8	1.977(3)	Na4–Cl1	2.882(2)
Se5–O10	1.687(3)	Cu4–O15	1.978(3)	Na4–Cl2	2.859(2)
Se5–OH5	1.763(3)	Cu4–O3	1.988(3)		
Se5–Cl2	3.3627(11)	Cu4–Cl3	2.7199(10)	Na5–Na5[a]	1.274(8)
Se5–Cl2	3.6282(11)	Cu4–Cl1	2.7884(10)	Na5–OH2	2.213(5)
				Na5–OH2	2.330(5)
Se6–O11	1.685(3)			Na5–O11	2.500(5)
Se6–O12	1.688(3)			Na5–O12	2.757(5)
Se6–OH6	1.765(3)			Na5–Cl3	2.932(4)
Se6–Cl1	3.4449(11)			Na5–Cl3	2.935(4)
Se6–Cl1	3.5728(11)				
Se7–O13	1.685(3)				
Se7–O14	1.698(3)				
Se7–OH7	1.769(3)				
Se7–Cl2	3.4866(11)				
Se7–Cl2	3.6008(11)				
Se8–O15	1.683(3)				
Se8–O16	1.694(3)				
Se8–OH8	1.773(3)				
Se8–Cl1	3.4270(11)				

[a]Na5 site s.o.f. = 50%.

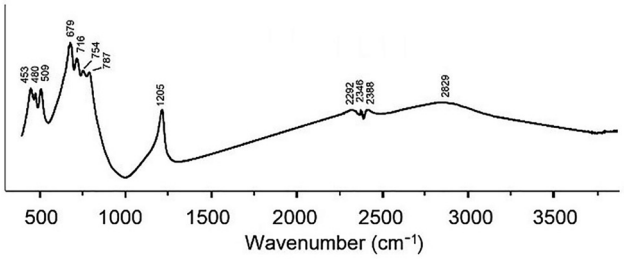

Figure 2: Infrared absorption spectra of **(NaCl)[Cu(HSeO$_3$)$_2$]-II**.

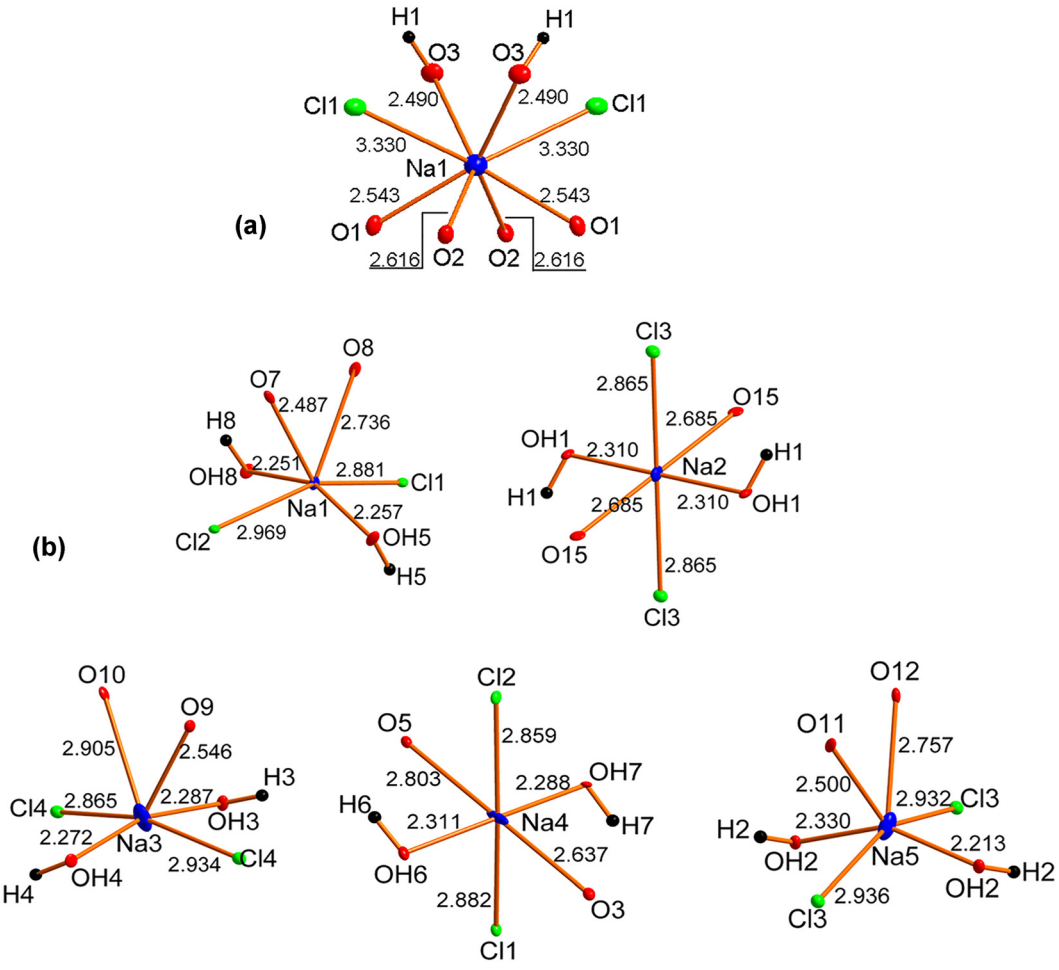

Figure 3: Coordination environments of Na^+ cations in (NaCl)[Cu(HSeO$_3$)$_2$]-**II** (a) and (NaCl)[Cu(HSeO$_3$)$_2$]-**III** (b). Displacement ellipsoids are drawn at the 50% probability level.

oxygen (two of which are protonated) and two chlorine atoms (d(Na–O) = 2.490(2)–2.617(2) Å, d(Na–Cl) = 3.3302(6) Å) (Figure 3a, Table 2).

The Cu^{2+} cation centers a [4+2] mixed-ligand CuO_4Cl_2 octahedron (Figure 4a), formed by a planar square with Cu–O distances in the range 1.976(1)–2.029(1) Å and two longer Cu–Cl apical bonds in the range 2.6058(9)–2.7765(9) Å. The structure of (NaCl)[Cu(HSeO$_3$)$_2$]-**II** (Figure 5a) is thus slightly different from that of (KCl)[Cu(HSeO$_3$)$_2$] (Figure 5b), wherein the Cu–Cl bond distances are 2.623(5) and 3.184(1) Å (Figure 4b), i.e. the Jahn-Teller distortion [23] of the CuO_4Cl_2 octahedron in the sodium compound is less pronounced. The likely reason is the size difference between K^+ and Na^+; in the former case, the distance between the [Cu(HSeO$_3$)$_2$] layers (Figure 4c and d) is longer and formation of Cu–Cl–Cu bridges is probably not possible at bonding distances to two Cu atoms. Also, the Cu···Cu distances within the [Cu(HSeO$_3$)$_2$] layer are longer in (KCl)[Cu(HSeO$_3$)$_2$] as compared to (NaCl)[Cu(HSeO$_3$)$_2$]-**II** (Figure 4c and d).

The selenium atoms reside in squashed SeO_3E tetrahedra; the dissimilarity in the Se–O distances is due to the protonation of one vertex of the SeO_3 group. The Se=O and Se–OH distances of 1.70 and 1.75 Å are only slightly longer and shorter, respectively, as observed for the other members of this family.

3.2 Cation coordination in (NaCl)[Cu(HSeO$_3$)$_2$]-III

In the more complex structure of (NaCl)[Cu(HSeO$_3$)$_2$]-**III** (Figure 6a), the five symmetrically independent Na^+ cations exhibit two different coordination environments (Figure 3b) which strongly differ from that observed in (NaCl)[Cu(HSeO$_3$)$_2$]-**II** (Figure 3a). The Na5 site is split over two positions with a 50% occupancy. The Na1, Na3, and Na5 atoms center irregular $NaO_2(OH)_2Cl_2$ polyhedra, whereas Na2 and Na4 atoms form distorted $NaO_2(OH)_2Cl_2$ octahedra. The Na–Cl

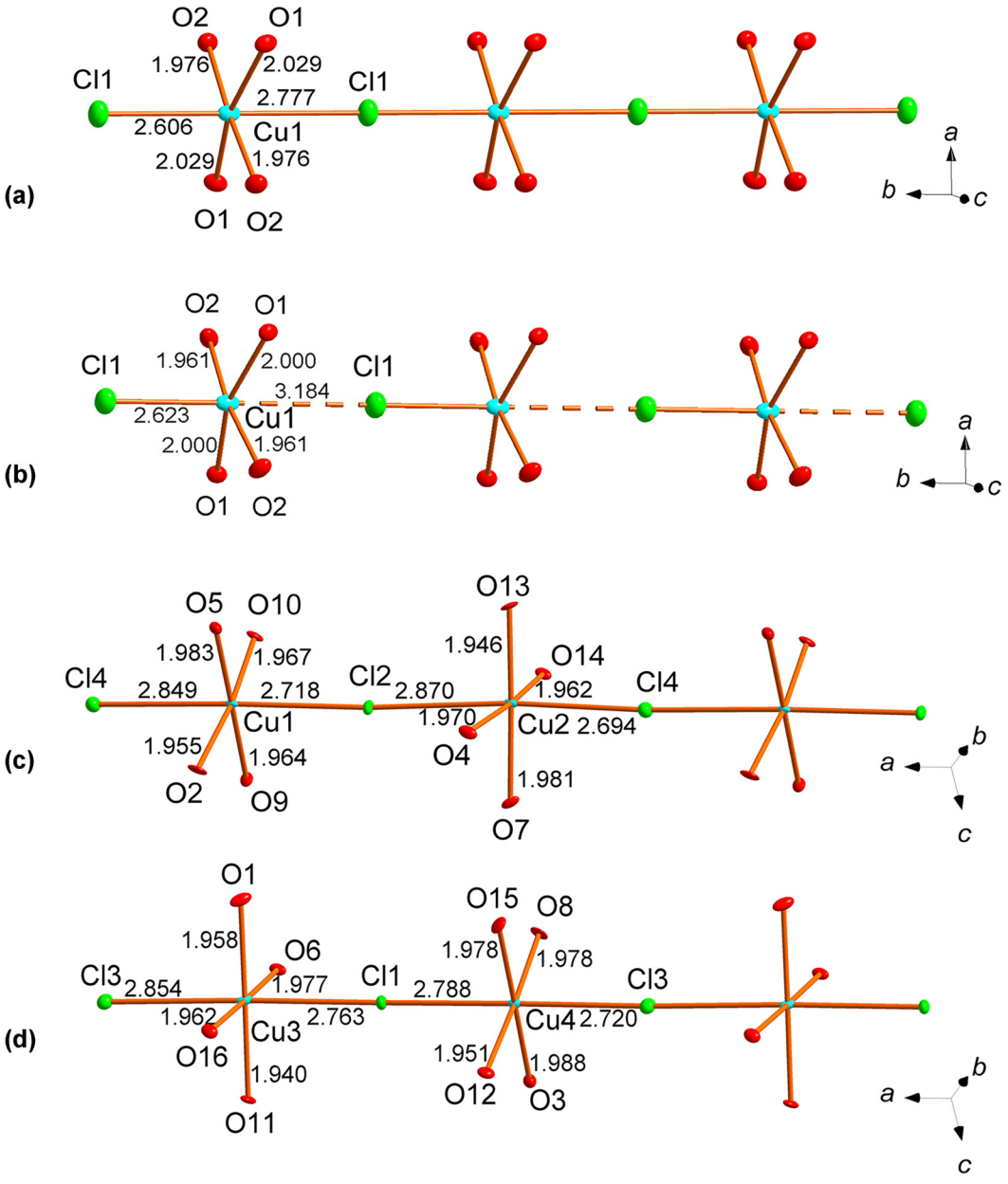

Figure 4: Cu^{2+} coordination environments in the structures of (NaCl)[Cu(HSeO$_3$)$_2$]-**II** (a), (KCl)[Cu(HSeO$_3$)$_2$] (Cu-Cl bonds > 3.0 Å are shown by dashed lines) (b) and (NaCl)[Cu(HSeO$_3$)$_2$]-**III** (c and d). Displacement ellipsoids are drawn at the 50% probability level.

bonds lie in the narrow range of 2.859(2)–2.969(2) Å which is notably less in comparison to 3.3302(6) Å observed in (NaCl)[Cu(HSeO$_3$)$_2$]-**II** (*vide supra*).

All four symmetrically independent Cu sites in (NaCl)[Cu(HSeO$_3$)$_2$]-**III** are coordinated by four oxygen atoms at similar Cu–O distances of ~1.95 Å forming planar CuO_4 squares complemented by two apical Cl^- (Figure 4c and d) to result in distorted CuO_4Cl_2 octahedra similar to those observed in (NaCl)[Cu(HSeO$_3$)$_2$]-**II**. The Cu–Cl bonds lie in the range of 2.694(1)–2.870(1) Å; the CuO_4Cl_2 octahedra share common Cl vertices forming chains shown in Figure 4c and d. Overall, the [Cu(HSeO$_3$)$_2$] layers in (NaCl)[Cu(HSeO$_3$)$_2$]-**III** (Figure 6b) demonstrate a new pattern of mutual orientation of the $HSeO_3^-$ groups not observed before among the other members of the (*AX*)[Cu(HSeO$_3$)$_2$] family [13].

4 Discussion

As noted above, (NaCl)[Cu(HSeO$_3$)$_2$]-**II** is isostructural to (KCl)[Cu(HSeO$_3$)$_2$]. However, there are essential differences in the environment of the Cu^{2+} cation. The coordination number of

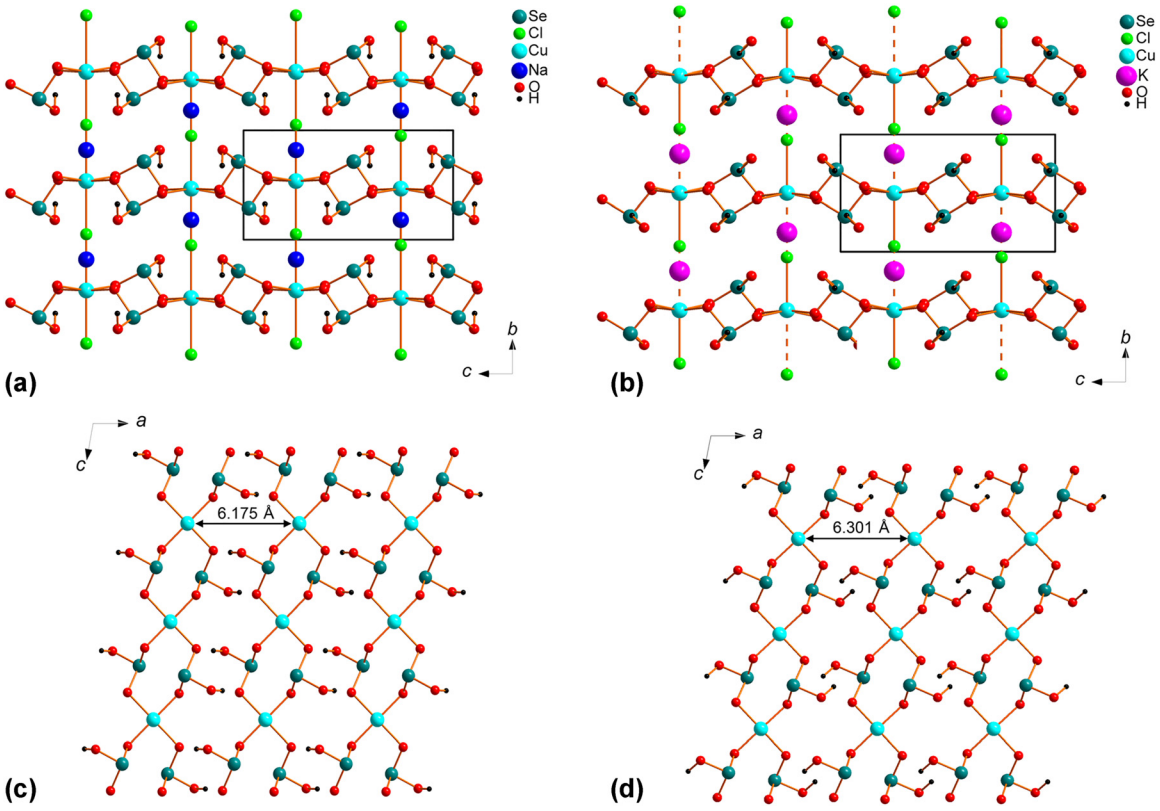

Figure 5: General projection of the crystal structure of (NaCl)[Cu(HSeO$_3$)$_2$]-**II** (a) and (KCl)[Cu(HSeO$_3$)$_2$] (Cu–Cl bonds > 3.0 Å are shown by dashed lines) (b). [Cu(HSeO$_3$)$_2$] layers (Cu^{2+} = blue balls; Se^{4+} = cyan balls; O^{2-} = red balls; H$^+$ = black balls) in (NaCl)[Cu(HSeO$_3$)$_2$]-**II** (c) and (KCl)[Cu(HSeO$_3$)$_2$] (d). Cu···Cu distance is enlarged in the latter, however general packing of HSeO$_3^-$ groups remains the same.

Cu^{2+} cation decreases with the increase of A$^+$ ionic radii, due to their size effect. As we had noted earlier [13], the structures of (*AX*)[Cu(HSeO$_3$)$_2$] compounds can be described as 3D [Cu(HSeO$_3$)$_2$Cl]$^-$ frameworks wherein the Cl$^-$ anions "stitch" the [Cu(HSeO$_3$)$_2$] layers and the voids are filled by alkali or ammonium cations. With the smallest Na$^+$, the Cu···Cu separations are evidently the shortest. In the structure of (KCl)[Cu(HSeO$_3$)$_2$], these separations are longer and the asymmetry of the copper coordination is increased. This situation can be considered intermediate between distorted octahedral and square-pyramidal coordination of Cu^{2+}. Finally, in [(RbCl)(Zn(HSeO$_3$)$_2$] [14] Zn^{2+} adopts a classical square pyramidal coordination, in line with its tendency to allow smaller coordination numbers compared to Cu^{2+}. It would be of interest if the same trend will be observed in the structures of yet unreported (*AX*)[Zn(HSeO$_3$)$_2$] compounds with *A* = K and Cs.

In both two new polymorphs of (NaCl)[Cu(HSeO$_3$)$_2$], their common feature is the formation of a copper-selenite substructure which is terminated by a 'lone-pair' shell facing chloride ions. The Se···Cl interactions seem to be important for the stabilization of the obtained structural architectures. The shortest Se···Cl contacts of 3.1474(4) Å are observed in the structure of (NaCl)[Cu(HSeO$_3$)$_2$]-**II** (Table 2). These distances are significantly longer in (NaCl)[Cu(HSeO$_3$)$_2$]-**III** and start from 3.366(1) Å observed for Se4···Cl4 (Table 3).

The structural architecture of (NaCl)[Cu(HSeO$_3$)$_2$]-**III** is rather similar to that of (NaCl)[Cu(HSeO$_3$)$_2$]-**I** [17] wherein the Na$^+$ cations occupy a disordered site. In the interlayer of (NaCl)[Cu(HSeO$_3$)$_2$]-**I** and (NaCl)[Cu(HSeO$_3$)$_2$]-**III** (Figure 6a), the lone electron pairs of Se^{IV} are associated forming micelles. Thus, the cavities in the 3D frameworks of these structures are filled in a checkerboard pattern by either sodium cations or lone electron pairs of Se^{IV}. Formation of such lone-pair micelles is not so evident in the structure of (NaCl)[Cu(HSeO$_3$)$_2$]-**II**.

The structure of (NaCl)[Cu(HSeO$_3$)$_2$]-**III** exhibits the most complex architecture among other [*M*$^{2+}$(HSeO$_3$)$_2$]-based structures. According to the chemical analysis and refinement results, K$^+$ is not incorporated; potassium is deposited instead at the first crystallization steps as the probably less soluble (KCl)[Cu(HSeO$_3$)$_2$] which does not incorporate noticeable amounts of Na$^+$, probably not the least due to the essential size difference between Na$^+$ and K$^+$. The sodium

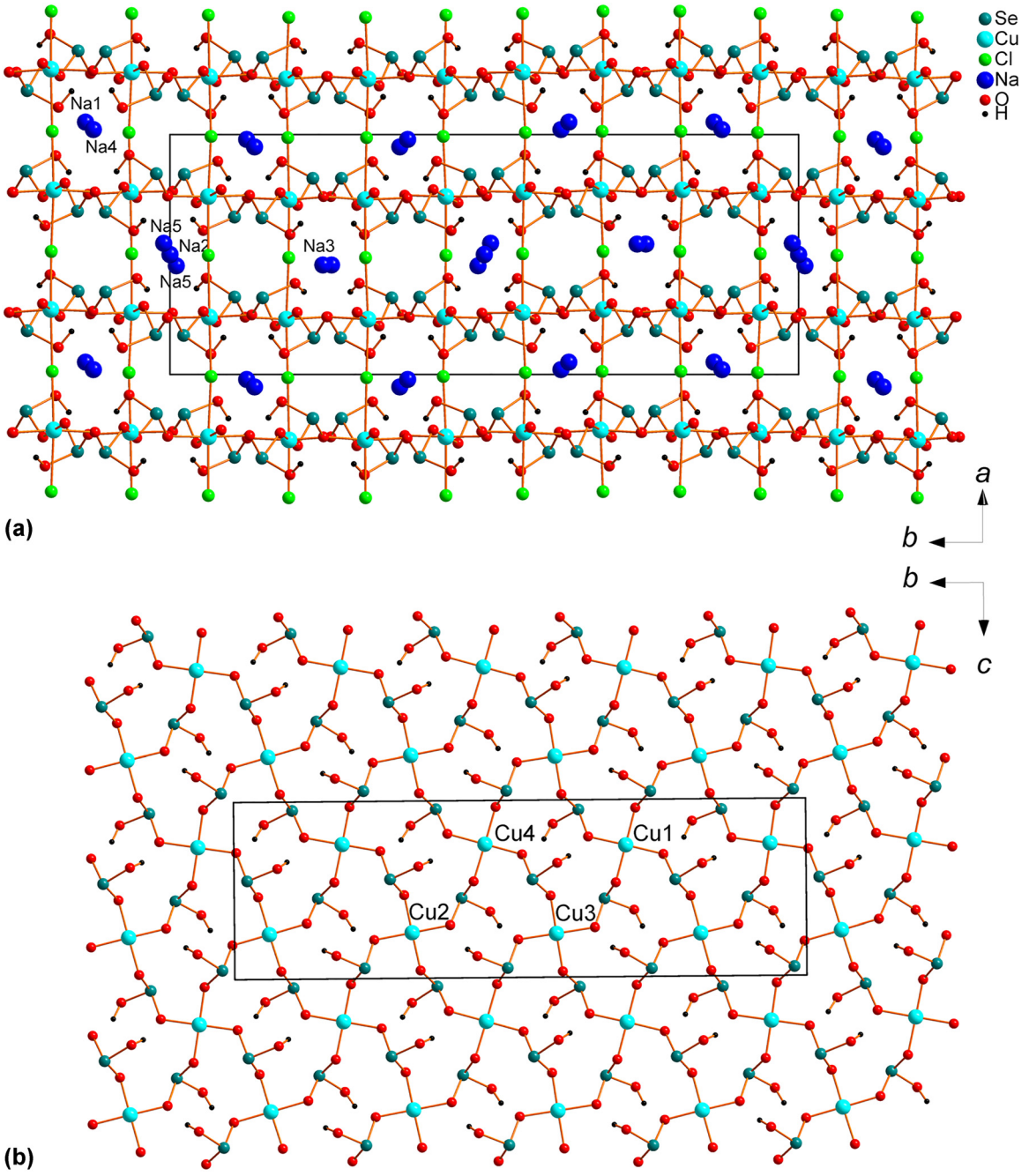

Figure 6: General projection of the crystal structure of (NaCl)[Cu(HSeO$_3$)$_2$]-**III** along the *c* axis (a) and [Cu(HSeO$_3$)$_2$] layer (b).

chloride-based system therefore seems to be the most structurally versatile; the relatively poor fit between the size of Na^+ and the $[Cu(HSeO_3)_2Cl]^-$ framework is likely to retard the crystallization and possibly makes it more sensitive to external factors like evaporation rate or presence of other species in the solution media. Note that according to the crystallization timescale, the polymorphs of (NaCl)[Cu(HSeO$_3$)$_2$] are formed in the order **I** < **III** < **II**. The structures of the polymorphs **I** and **III** are close but a slightly longer crystallization time of **III** (probably due to depletion of the mother liquor of Cu^{2+} and $HSeO_3^-$ due to precipitation of (KCl)[Cu(HSeO$_3$)$_2$] and low initial Na^+ content) promotes formation of a better-ordered motif corresponding to a well-developed superstructure. Finally, very long crystallization

time required for **II** leads to a fully ordered, while somewhat different, structure. It would be of interest to see if similar polymorphism could be observed in chemically related systems, e.g. AX – ZnX_2 or CdX_2 – H_2SeO_3.

Note also that different architectures were reported for two Co-based systems with a cation size-dependent hydration: $Cs_2[Co(HSeO_3)_2Cl_2]$ and $K_2(H_2O)_2[Co(HSeO_3)_2Cl_2]$ [24]. Therefore, the structural and chemical perspectives of the "layered hydroselenite" family are quite appealing, and even variation of purely inorganic interlayer "filling" will evidently produce new structural and probably magnetic phenomena. The problems yet to be overcome are the phase purity and reproducibility of the synthesis. As already noted, the presence of excess amounts of species aimed at the interlayer "filling" commonly leads to co-crystallization of other hydroselenite or halide selenite species; the low solubility of $CuSeO_3{\cdot}2H_2O$ permits its precipitation, as a by-phase, even in relatively strongly acidic media [9, 13]. Several successful cases are reported for the ethylenediammonium-templated species in organic media [11]; this approach is not fully appropriate for purely inorganic syntheses as the solubility of inorganic salts in common organic solvents is generally low. Investigations are currently underway at finding the exact synthesis conditions for the new members of this intriguing family.

Acknowledgements: We are grateful to Uwe Kolitsch and one anonymous reviewer for valuable comments. Technical support by the X-Ray Diffraction and Microscopy and Microanalysis Resource Centers of Saint-Petersburg State University is gratefully acknowledged.

Author contributions: All the authors have accepted responsibility for the entire content of this submitted manuscript and approved submission.

Research funding: None declared.

Conflict of interest statement: The authors declare no conflicts of interest regarding this article.

References

1. Asai T., Kiriyama R. Optical and magnetic studies of $CuSeO_3(H_2O)_2$ based on the refined crystal structure. *Bull. Chem. Soc. Jpn.* 1973, *46*, 2395.
2. Berdonosov P. S., Janson O., Olenev A. V., Krivovichev S. V., Rosner H., Dolgikh V. A., Tsirlin A. A. Crystal structures and variable magnetism of $PbCu_2(XO_3)_2Cl_2$ with X = Se, Te. *Dalton Trans.* 2013, *42*, 9547–9554.
3. Tellgren R., Liminga R. Hydrogen bond studies. LXXXVII. A neutron diffraction study of ammonium trihydrogen selenite. *Acta Crystallogr.* 1974, *B30*, 2497–2499.
4. Vinorgadova I. S. ^{2}D and ^{133}Cs NMR study of the hydrogen bond network and antiferroelectric. *J. Solid State Chem.* 1981, *40*, 361–368.
5. Shuvalov L. A., Bondarenko V. V., Varikash V. M., Gridnev S. A., Makarova I. P., Simonov V. I. Thallium-tri-hydrogen selenite, $TlH_3(SeO_3)_2$ – a new member of alkaline tri-hydrogen selenite crystal family. *Ferroelectrics Lett.* 1984, *2*, 143–146.
6. Sheldrick W. S., Häusler H.-J. Das Hydrogendiarsenit-Anion $HAs_2O_5^{3-}$. Darstellung und Struktur von $K_3HAs_2O_5{\cdot}6H_2O$. *Z. Naturforsch.* 1985, *40b*, 1622–1625.
7. Sheldrick W. S., Häusler H.-J. Zur Kenntnis von Natriumarseniten im Dreistoffsystem Na_2O – As_2O_3 – H_2O bei 6°C. *Z. Anorg. Allg. Chem.* 1987, *549*, 177–186.
8. Effenberger H., Miletich R., Pertlik F. Structure of dilead(II) hydrogenarsenate(III) dichloride. *Acta Crystallogr.* 1990, *C46*, 541–543.
9. Markovski M. R., Siidra O. I., Charkin D. O., Nazarchuk E. V., Grishaev V. Yu. Molecular inorganic polymers: synthesis and crystal structures of $KCl{\cdot}2H_2SeO_3$ and $CsCl{\cdot}H_2SeO_3$. *Z. Kristallogr.* 2020, *235*, 553–557.
10. Baran J., Lis T., Marchewka M., Ratajczak H. Structure and polarized IR and Raman spectra of $Na_2SeO_4{\cdot}H_2SeO_3{\cdot}H_2O$ crystal. *J. Mol. Struct.* 1991, *250*, 13–45.
11. Feng M.-L., Prosvirin A. V., Mao J.-G., Dunbar K. R. Syntheses, structural studies, and magnetic properties of divalent Cu and Co selenites with organic constituents. *Chem. Eur. J.* 2006, 8312–8323.
12. Markovski M. R., Charkin D. O., Siidra O. I., Nekrasova D. O. Copper hydroselenite nitrates $(A^+NO_3)_n[Cu(HSeO_3)_2]$ (A = Rb$^+$, Cs$^+$ and Tl$^+$, n = 1, 2) related to Ruddlesden – Popper phases. *Z. Kristallogr.* 2019, *234*, 749–756.
13. Charkin D. O., Markovski M. R., Siidra O. I., Nekrasova D. O., Grishaev V. Yu. Influence of the alkali cation size on the Cu^{2+} coordination environments in (AX)[Cu($HSeO_3$)$_2$] (A = Na, K, NH_4, Rb, Cs; X = Cl, Br) layered copper hydrogen selenite halides. *Z. Kristallogr.* 2019, *234*, 739–747.
14. Spirovski F., Wagener M., Stefov V., Engelen B. Crystal structures of rubidium zinc bis (hydrogenselenate (IV)) chloride $RbZn(HSeO_3)_2Cl$, and rubidium zinc bis (hydrogenselenate (IV)) bromide $RbZn(HSeO_3)_2Br$. *Z. Kristallogr. NCS* 2007, *222*, 91.
15. Trombe J. C., Lafront A. M., Bonvoisin J. Synthesis, structure and magnetic measurement of a new layered copper hydrogenselenite: $(Cu(HSeO_3)_2){\cdot}((NH_4)Cl)$. *Inorg. Chim. Acta* 1997, *262*, 47.
16. Markovski M. R., Siidra O. I., Charkin D. O., Grishaev V. Y. Layered calcium hydrogen selenite chlorides $Ca(HSeO_3)Cl$ and $Ca(HSeO_3)Cl(H_2O)$, the first halides obtained in $CaCl_2$–H_2SeO_3–H_2O system. *Z. Kristallogr.* 2020, *235*, 439–443.
17. Kovrugin V. M., Krivovichev S. V., Mentré O., Colmont M. [NaCl][Cu($HSeO_3$)$_2$], NaCl-intercalated $Cu(HSeO_3)_2$: synthesis, crystal structure and comparison with related compounds. *Z. Kristallogr.* 2015, *230*, 573–577.
18. Sheldrick G. M. Crystal structure refinement with SHELXL. *Acta Crystallogr.* 2015, *A71*, 3.
19. Berger J. Infrared and Raman spectra of $CuSO_4$, $5H_2O$; $CuSO_4$, $5D_2O$; and $CuSeO_4$, $5H_2O$. *J. Raman Spectrosc.* 1976, *5*, 103–114.
20. Kretzschmar J., Jordan N., Brendler E., Tsushima S., Franzen C., Foerstendorf H., Brendler V., Heim K. Spectroscopic evidence for selenium (IV) dimerization in aqueous solution. *Dalton Trans.* 2015, *44*, 10508–10515.
21. Valkonen J. Crystal structures, infrared-spectra, and thermal behavior of calcium hydrogenselenite monohydrate $Ca(HSeO_3)_2H_2O$, and

dicalcium diselenite bis(hydrogenselenite) $Ca_2(HSeO_3)_2(Se_2O_5)$. *J. Solid State Chem.* 1986, *65*, 363–369.
22. Nakamoto K. *Infrared and Raman Spectra of Inorganic and Coordination Compounds, Part B, Applications in Coordination, Organometallic, and Bioinorganic Chemistry*; John Wiley and Sons: Hoboken, 2009; p. 54.
23. Jahn H. A., Teller E. Stability of polyatomic molecules in degenerate electronic states. *Proc. R. Soc. London, Ser.* 1937, *A161*, 220.
24. Wagener M. Synthese, Charakterisierung und strukturchemische Aspekte von Kupfer-und Silberchalkogenohalogeniden sowie von Halogeno-und Oxochalkogenaten (IV), 2005. Dissertation, Siegen. https://d-nb.info/97663936X/34.

Supplementary Material: This article contains supplementary material (https://doi.org/10.1515/zkri-2023-0004).